The flare-in texture in rotating superfluid ^{3}He-B

1990 J. Phys.: Condens. Matter 2 1325

(http://iopscience.iop.org/0953-8984/2/5/023)

J. Phys.: Condens. Matter **2** (1990) 1325–1333. Printed in the UK

The flare-in texture in rotating superfluid ^{3}He-B

M M Salomaa

Low Temperature Laboratory, Helsinki University of Technology, SF-02150 Espoo 15, Finland

Received 16 March 1989, in final form 4 September 1989

Abstract. A new first-order phase transition is proposed to manifest itself in rotating ^{3}He-B for the vortex-free state, owing to counterflow. The 'flare-out' texture is found to become spontaneously unstable towards a new 'flare-in' texture, which is suggested to explain the transition, first observed with the use of NMR by Hakonen and Nummila in 1987 and confirmed by Korhonen and co-workers in 1989, to a previously unidentified state characterised by a signal corresponding to $\beta = 90°$, i.e., with a vector $\hat{\boldsymbol{n}}$ perpendicular to $\boldsymbol{H} \parallel \boldsymbol{\Omega} \parallel \hat{\boldsymbol{z}}$. This transition is also expected to be observable in other experiments, such as ones based on ultrasonic measurements, on the vortex-free state of rotating superfluid ^{3}He-B, a new tenfold splitting of the real squashing mode is predicted to occur for the flare-in texture.

1. Introduction

NMR experiments on the rotating A and B phases of ^{3}He gave rise to the discovery of quantised vortex lines in these exotic superfluids (for recent experimental and theoretical reviews, see Hakonen *et al* 1989b, Salomaa and Volovik 1987, respectively). The flare-out $\hat{n}$ texture (Brinkman *et al* 1974, Smith *et al* 1977, Spencer and Ihas 1982), which exists in superfluid ^{3}He-B in a cylinder for an axial magnetic field, is modified by vortices (Gongadze *et al* 1981) in the rotating equilibrium state; this results in a smooth change of the $\hat{\boldsymbol{n}}$ texture, which is reflected in the spin-wave spectrum (Maki and Nakahara 1983, Hakonen and Volovik 1982, Theodorakis and Fetter 1983, Jacobsen and Smith 1983, Hakonen *et al* 1989a) localised on the flare-out-like texture.

In this paper, I consider a different, discontinuous, textural effect which has been observed in rotating ^{3}He-B. In the first NMR experiments (Hakonen *et al* 1983), a vortex-free state was obtained immediately after the start of rotation. This texture was believed to be just a transient one which could only exist for about one minute after the start of rotation, prior to the ^{3}He vortices being nucleated. However, recent experiments (Hakonen and Nummila 1987) have amply demonstrated that the vortex-free state can be made to persist for an arbitrarily long time for angular velocities less than a critical value, $\Omega < \Omega^*$, which depends on pressure, temperature and the direction of rotation. The experimental cell, having smooth walls, was equipped with a Mylar diaphragm possessing a 1.5 mm hole; the latter was installed in order to separate the cylindrical (radius R) sample from the heat-exchanger volume, whereby vortex formation in the NMR volume became strongly inhibited.

Hakonen and Nummila reported two interesting phenomena in the vortex-free state, in the presence of a normal liquid versus superfluid counterflow: (i) an asymmetry of

0953-8984/90/051325+09$03.50

the spin-wave spectrum with respect to reversal of the sense of rotation, $\boldsymbol{\Omega} \longleftrightarrow -\boldsymbol{\Omega}$, even though there were no vortices present (with consequent ferromagnetic cores, thus possibly giving rise to a gyromagnetic effect; cf Salomaa and Volovik 1987); and (ii) the appearance, for $\Omega > \Omega^*$, of a new, narrow peak in the NMR spectrum, corresponding to $\sin^2\beta = 1$, i.e., with $\beta = 90°$ (cf equation (2)). More recent experiments by Korhonen *et al* (1989), with a somewhat different geometry, have not reproduced the (small) asymmetry, but have further confirmed the sharp $\sin^2\beta = 1$ feature in the NMR spectrum and helped to clarify the metastabilities in its occurrence.

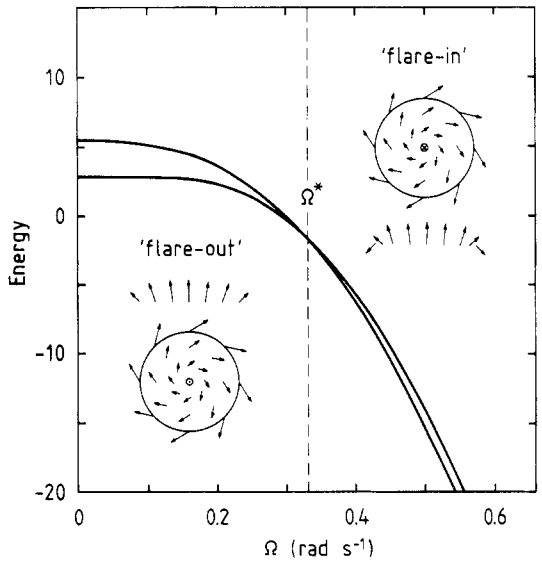

Figure 1. The computed energies for the two depicted vortex-free $\hat{\boldsymbol{n}}$-vector textures as functions of Ω, the angular velocity of rotation: the conventional flare-out texture, with $\hat{\boldsymbol{n}}(r = 0) \parallel \hat{\boldsymbol{\Omega}}$, occurs for $\Omega < \Omega^* = 0.331$ rad s^{-1}. The new flare-in texture, with $\hat{\boldsymbol{n}}(r = 0) \parallel -\hat{\boldsymbol{\Omega}}$, is here found to be energetically more favourable for $\Omega > \Omega^*$. The countercurrent-driven transition between these two textures is of first order, thus explaining the experimentally investigated metastability. In all figures I have chosen parameters appropriate at $p = 10.3$ bar, $T = 0.58\,T_c$ and $H = 27.3$ mT (cf figure 4).

It has been suggested (Salomaa and Volovik 1989) that the first effect, i.e. the spin-wave asymmetry, would arise from a possible A-phase surface layer (Thuneberg 1986) on bulk ^{3}He-B. The second effect, an NMR signal at $\beta = 90°$, is here first proposed to arise through a first-order phase transition, see figure 1, between two distinct textures with the same axial and discrete symmetries, but possessing different real-space topologies. This appears to account well for the measured NMR spectra.

2. The flare-out texture

The B-phase order parameter is an orthogonal matrix with elements $R_{\alpha i}$ which describes the rotation of the spin system with respect to the orbital quantisation axis through the 'magic' angle $\theta_0 = \cos^{-1}(-\frac{1}{4})$ about the axis $\hat{\boldsymbol{n}}$. The conventional $\hat{\boldsymbol{n}}$-vector distribution in a straight cylinder, for an axial magnetic field, is the so-called flare-out texture with

$$R_{\alpha i} = \cos\theta_0\,\delta_{\alpha i} + (1 - \cos\theta_0)n_\alpha n_i - e_{\alpha ik}n_k \sin\theta_0 \qquad (1)$$

where

$$\hat{\boldsymbol{n}}(r, \varphi) = \hat{\boldsymbol{z}} \cos \beta(r) + \sin \beta(r)(\hat{\boldsymbol{\varphi}} \sin \alpha(r) - \hat{r} \cos \alpha(r)). \tag{2}$$

Here r, φ and z denote the cylindrical coordinates, and $\alpha(r)$ and $\beta(r)$ specify the local orientation of the $\hat{\boldsymbol{n}}$ vector.

On the walls of the cylinder, the boundary condition for $\hat{\boldsymbol{n}}$ is imposed by the surface magnetic anisotropy energy:

$$F_{\text{surf}} = -d\,(H_\alpha R_{\alpha i} \hat{\nu}_i)^2 \tag{3}$$

where $\hat{\boldsymbol{\nu}}$ is normal to the cylinder wall. A minimisation of this surface energy produces four different sets of boundary conditions at the radius $r = R$:

$$\hat{\boldsymbol{n}}^{(a)}(R, \varphi) = \frac{1}{\sqrt{5}}(\sigma_z^{(a)} \hat{\boldsymbol{z}} + \sigma_r^{(a)} \hat{r} + \sqrt{3}\sigma_\varphi^{(a)} \hat{\boldsymbol{\varphi}}) \tag{4}$$

where $a = 1, 2, 3, 4$, with the signatures $\boldsymbol{\sigma}^{(1)} = (+, +, -)$, $\boldsymbol{\sigma}^{(2)} = (+, -, +)$, $\boldsymbol{\sigma}^{(3)} = (-, +, +)$ and $\boldsymbol{\sigma}^{(4)} = (-, -, -)$. This gives four degenerate axisymmetric $\hat{\boldsymbol{n}}$ textures which may be transformed into each other through symmetry operations (cf figure 2 of Salomaa and Volovik 1989), thus manifesting the symmetry breaking induced by the boundary conditions which are here taken as rigid; this serves to illustrate the basic mechanism for the new phase transition.

3. The flare-in texture

Numerical calculations of the $\hat{\boldsymbol{n}}$ texture with rigid boundary conditions usually take into account only the conventional flare-out texture (Spencer and Ihas 1982, Volovik *et al* 1982, Hakonen *et al* 1983, 1989a, Salomaa and Volovik 1989, Nummila *et al* 1989), characterised by the variation of β between 0° and 63.4°, but overlook the possibility of another solution whose energy is also a local minimum in the configuration space. This competing flare-in texture is characterised by the range of variation in $\beta > 90°$; I have also computed the latter $\hat{\boldsymbol{n}}$-vector textures.

In the bulk B phase, the magnetic anisotropy free energy is given by (following experimental arrangements, I choose an axial magnetic field $\hat{\boldsymbol{z}}$: $H_k = H\hat{z}_k$):

$$F_{\text{H}} = -a(\hat{\boldsymbol{n}} \cdot \boldsymbol{H})^2. \tag{5}$$

The superfluid–normal liquid countercurrent

$$\boldsymbol{w} = \boldsymbol{v}_s - \boldsymbol{v}_n = -\boldsymbol{\Omega} \times \boldsymbol{r} \tag{6}$$

present in the vortex-free state, gives rise to the free-energy term

$$F_{\text{flow}} = -\tfrac{2}{5} a(w_i R_{ik} H_k)^2 / v_{\text{D}}^2 \tag{7}$$

where the dipolar critical velocity, $v_{\text{D}} = 0.30\ \text{mm s}^{-1}$, is obtained by interpolation from recent measurements (Nummila *et al* 1989). The gradient free energy is given by

$$F_{\text{G}} = \tfrac{16}{13} c \left[(\nabla_i \hat{\boldsymbol{n}})^2 - \tfrac{1}{2} \left(\sqrt{\tfrac{5}{8}} \hat{\boldsymbol{n}} \cdot \nabla \times \hat{\boldsymbol{n}} + \sqrt{\tfrac{3}{5}} \nabla \cdot \hat{\boldsymbol{n}} \right)^2 \right] \tag{8}$$

where the parameter $c = aH^2\xi_H^2$, with the magnetic healing length ξ_H, for which I use the data of Hakonen *et al* (1989a); hence there are *no free parameters in the present calculation.*

Inserting the representation (2) for $\hat{\boldsymbol{n}}$ into (5), (7) and (8) gives the following minimisation problem for $\alpha(r)$ and $\beta(r)$:

$$F = \tfrac{16}{13}\, c\, 2\pi R^2 \int_0^1 r\,\mathrm{d}r \left\{ (\beta')^2 + \sin^2\beta\,(\alpha')^2 + \frac{\sin^2\beta}{r^2} - \tfrac{1}{2}\left[\left(\sqrt{\tfrac{5}{8}}\sin\alpha - \sqrt{\tfrac{3}{8}}\cos\alpha\cos\beta \right)\beta' \right.\right.$$
$$+ \left(\sqrt{\tfrac{5}{8}}\sin\alpha\cos\beta - \sqrt{\tfrac{3}{8}}\cos\alpha \right)\frac{\sin\beta}{r} + \left(\sqrt{\tfrac{5}{8}}\cos\alpha\cos\beta + \sqrt{\tfrac{3}{8}}\sin\alpha \right)\sin\beta\alpha' \left.\right]^2$$
$$\left. + \frac{R^2}{(\xi_H')^2}\sin^2\beta \left[1 - \left(\frac{R}{r_\Omega} \right)^2 r^2 \left(\sqrt{\tfrac{5}{8}}\sin\alpha\cos\beta - \sqrt{\tfrac{3}{8}}\cos\alpha \right)^2 \right] \right\} \qquad (9)$$

where $\alpha' \equiv (\mathrm{d}\alpha/\mathrm{d}r)$, $\beta' \equiv (\mathrm{d}\beta/\mathrm{d}r)$, $\xi_H' \equiv (\frac{16}{13})^{1/2}\xi_H$ (cf Hakonen *et al* 1989a), and $r_\Omega = v_D/\Omega$; here I use $R = 3.5$ mm in the computations, to comply with the latest experimental cell. The minimisation problem posed by (9) was first solved by Volovik *et al* (1982), but only for the flare-out-like $\hat{\boldsymbol{n}}$ textures. Here I have included also the flare-in structures. The resulting free energies for these two competing textures are shown in figure 1 as functions of Ω. For brevity, all calculations presented here are performed with parameters appropriate at $p = 10.3$ bar, $H = 27.3$ mT and $T = 0.58\,T_c$ to facilitate comparison with the data given later (see figure 4).

The critical angular velocity obtained, $\Omega^\star = 0.331$ rad s^{-1}, is in a remarkably good agreement with the critical rotation speeds for which the sharp peak at $\sin^2\beta = 1$ first appears: in the experiments of Korhonen *et al* (1989), $\Omega_+^\star \simeq 0.35$ rad s^{-1} upon acceleration and $\Omega_-^\star \simeq 0.24$ rad s^{-1} during deceleration fall just above and below the theoretical estimate, respectively. Presumably, due to the hysteretic character of the first-order transition, one ought rather to compare equilibrium energies with the average value, $\frac{1}{2}(\Omega_+^\star + \Omega_-^\star) \simeq 0.30$ rad s^{-1}. Moreover, the present, very simple, textural calculation does not account for the possible small additional surface energies (cf Salomaa and Volovik 1989), but such contributions are not quantitatively well known at present. Changing the value of v_D from 0.30 mm s^{-1} (experimental estimate) to 0.24 mm s^{-1} (theoretical estimate) only shifts the computed transition from $\Omega^\star = 0.331$ rad s^{-1} to $\Omega^\star = 0.264$ rad s^{-1}, which is still in fair agreement with the measured values under the same conditions. One obtains a fair estimate for the measured hysteresis in Ω by taking the textural transition to occur where the energy surplus (textural energy difference between the flare-out and the flare-in configurations) corresponds to the energy, according to (5), required to reverse $\hat{\boldsymbol{n}}$ in the appropriate volume.

Figures 2 display the computed dependence of the angles $\alpha(r)$ and $\beta(r)$ on the angular velocity of rotation for the two possible rotating vortex-free counterflow states of ^{3}He-B. For the flare-out-like textures, in particular, I want to point out the large gradients induced in $\beta(r)$ and $\alpha(r)$ for $r \to R$ when $\Omega \geq \Omega^\star = 0.331$ rad s^{-1}; note how $\beta(r)$ bends over twice, becoming double-valued near the wall. In contrast to the flare-out-like texture, the countercurrent peak for the flare-in NMR spectrum does not split since $\beta(r)$ in figure 2(*b*) remains single-valued everywhere. The flare-in textures display a smooth behaviour for $\alpha(0 \leq r \leq R)$ and, especially, for the value of $\beta(r \to R)$ that results in a considerable reduction in the gradient free energy, equation (8), of the flare-in texture near the walls in comparison with that of the flare-out texture.

This explains the crossing of the textural energies at $\Omega = 0.331$ rad s^{-1}. It is interesting, in particular, to compare the angles $\alpha(r)$ and $\beta(r)$ for the two textures

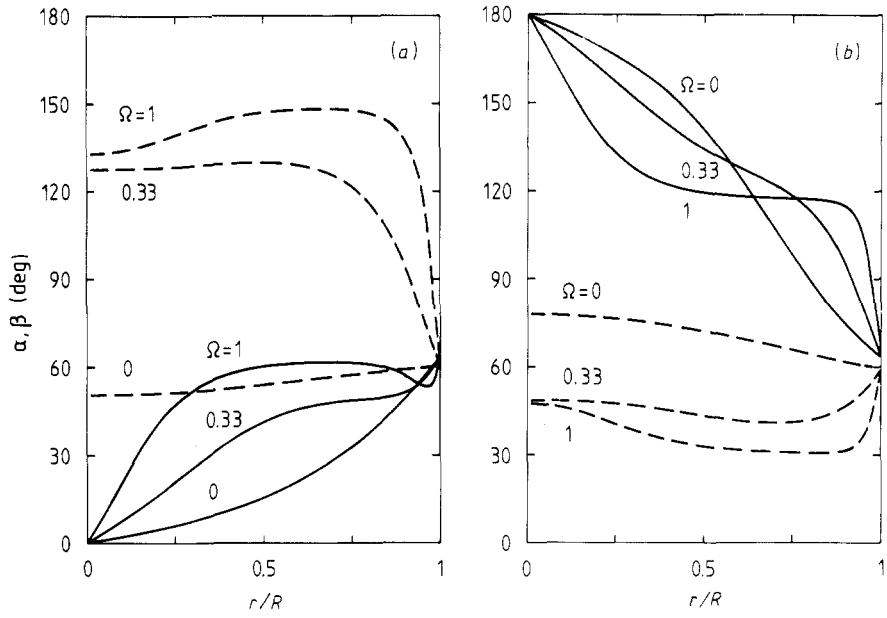

Figure 2. Radial distributions for the $\hat{\boldsymbol{n}}$-textural angles α (broken curve) and β (full curve), defined in equation (2), as functions of Ω (in rad s^{-1}) for the vortex-free textures in ^{3}He-B. (*a*) The flare-out texture. (*b*) The flare-in texture.

at $\Omega = 1$ rad s^{-1}: up to the transformations $\beta^{\text{flare-in}} = \pi - \beta^{\text{flare-out}}$ and $\alpha^{\text{flare-in}} = \pi - \alpha^{\text{flare-out}}$, the curves are to all intents and purposes the same in the bulk region; a difference only appears in a narrow shell in the vicinity of the walls, where the countercurrent-induced textural reversal of $\hat{\boldsymbol{n}}$ takes place.

4. The NMR signature of the flare-in texture

The angle β between $\hat{\boldsymbol{n}}$ and $\boldsymbol{H}$ determines the shift of the NMR resonance frequency ω with respect to the Larmor frequency ω_0 in transverse NMR (Leggett 1973, Osheroff 1977):

$$\omega - \omega_0 = \left(\frac{\Omega_L^2}{2\omega_0}\right) \sin^2 \beta \tag{10}$$

where $\Omega_L \ll \omega_0$ is the Leggett frequency. Here I am not interested in the individual positions of the NMR absorption peaks, but rather in the overall lineshape of the power spectrum $P(\omega)$ thus I may apply the local-oscillator approximation:

$$P(\omega) = \frac{2}{R^2} \int_0^R \mathrm{d}r\, r\, \delta(\omega - \omega(r)) \propto \left(\frac{\partial \sin^2 \beta}{\partial r^2}\right)^{-1} \tag{11}$$

where the local NMR frequency $\omega(r)$ is given by (10). The computed $P(\omega)$ is displayed in figure 3. For $\Omega = 0$ in figure 3(*a*), the flare-out lineshape is characterised by a sharp absorption maximum at the Larmor frequency ω_0, corresponding to $\sin^2 \beta = 0$. For larger Ω, such as $\Omega = 0.33$ rad s^{-1} in figure 3(*b*), the centre-of-mass of the spectrum

shifts towards higher frequencies. At the critical value $\Omega = \Omega^*$, the counterflow peak (Volovik *et al* 1982) appears very pronounced. On further increasing Ω, there would emerge Van Hove singularities in $P(\omega)$ which would follow from the two extrema in $\sin^2\beta(r)$ near the wall; see the curve for $\Omega = 1$ rad s^{-1} in figure 2(*a*). However, the textural phase transition occurs, according to the present calculation, from the flare-out into the flare-in texture—characterised in NMR spectra by a signature like the one in figure 3(*c*)—just where $\beta(r)$ would become double-valued; the texture transforms in order to diminish the gradient energy.

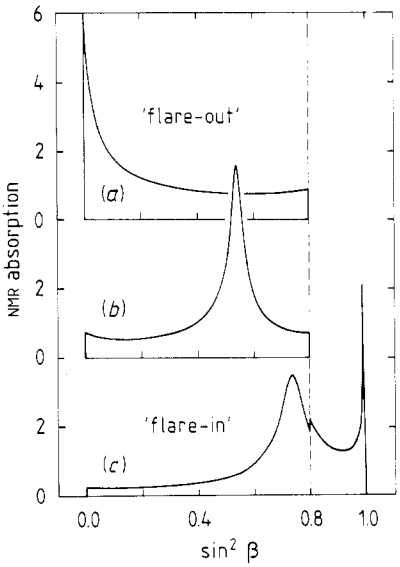

Figure 3. The spectral distribution of the NMR absorption, $P(\omega)$, clearly manifests the textural transition from the flare-out into the flare-in configuration. The calculated NMR signatures for the flare-out-like textures are for (*a*) $\Omega = 0$ and (*b*) $\Omega = 0.33$ rad s^{-1}; note the countercurrent-induced peak in the latter spectrum. (*c*) The computed NMR signal for the new flare-in texture at $\Omega = 0.5$ rad s^{-1}. Note, in particular, the sharp peak in the signal for $\beta = 90°$; this serves as the flare-in 'fingerprint' in NMR. Moreover, the signal is characterised by an appreciably broadened counterflow peak which is shifted towards $\sin^2\beta = 0.8$.

Figure 4 displays experimental NMR spectra measured at the same temperature ($T = 0.58\ T_c$), pressure ($p = 10.3$ bar), and field ($H = 27.3$ mT) for which the calculations in figure 3 were performed. One finds that the overall features are rather well described by the proposed flare-out↔flare-in textural transition. In particular, the appearance of the sharp peak at $\sin^2\beta = 1$ and its shape (allowing for broadening due to finite experimental resolution) are well reproduced without any fitting parameters.

Hakonen and Nummila (1987) also discovered events where $\sin^2\beta$ was slightly less than 1.0 for the sharp new feature. This can be readily accounted for on the basis of figure 2(*b*): it is to be expected that the boundary conditions on the cylindrical surface ought not be considered absolutely rigid, but rather that the textural angles $\alpha(r = R)$ and $\beta(r = R)$ should be allowed to slip, thus assuming values that would at once *minimise the total textural energy*: $F_{\text{bulk}} + F_{\text{surface}}$. Other anomalous cases were reported as well, such as one or two peaks below $\sin^2\beta = 1$, accompanying the 90° signal. We suggest that these additional features should not be taken as evidence for yet other,

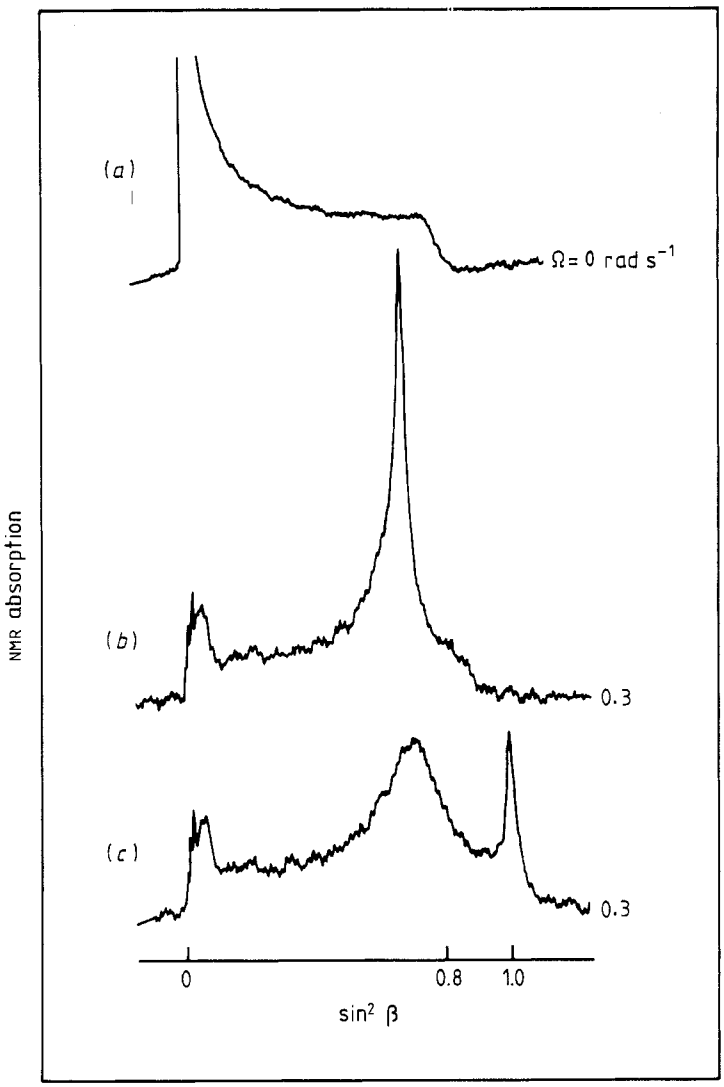

Figure 4. The measured NMR spectrum as a function of the normalised frequency shift (according to Korhonen *et al* 1989). The two lineshapes on the top are interpreted as corresponding to the regular flare-out-like textures, while the spectrum at the bottom is suggested to signal the occurrence of the flare-in-like $\hat{\boldsymbol{n}}$-vector texture.

more complicated textures, but that they could possibly be accounted for instead by a spectrum of bound spin waves on the present texture, localised not in the centre but near the wall, and determined as the eigensolutions of the Schrödinger-like spin-wave equation (Hakonen and Volovik 1982, Hakonen *et al* 1989a).

5. Discussion

One should next compute the spectrum of bound spin waves localised near the wall for the textures considered here and study them further by adjusting $\alpha(R)$ and $\beta(R)$.

While such work, both experimental and computational, is necessary in order to study the textural and the possible surface transitions in quantitative detail, it is not expected to change the qualitatively important new result: the vortex-free $\hat{\boldsymbol{n}}$ texture in rotating superfluid ^{3}He-B undergoes a spontaneous first-order phase transition between the flare-out and the flare-in textures.

I hope that the present work will serve to help in elucidating the NMR data (Hakonen and Nummila 1987, Korhonen *et al* 1989) on rotating ^{3}He-B in the vortex-free states. One should also evaluate the real squashing (RSQ) mode spectra for the flare-out (fivefold splitting in an external magnetic field) and the flare-in (tenfold splitting) textures, so that the doubling in the number of the resonant RSQ-mode peaks could be utilised for identification in the ultrasonic measurements on rotating superfluid ^{3}He-B (Salmelin *et al* 1989), just as the peak at $\beta = 90°$ in figure 3 provides a method for recognising the new flare-in texture via NMR.

The flare-out texture (just like the Mermin–Ho texture for $\hat{\boldsymbol{l}}$ in the A phase) may be visualised as an escape of $\hat{\boldsymbol{n}}$ into the third dimension. The transition between the flare-out and flare-in textures provides an example of the novel situation where the 'escape into the third dimension' can flip between the two different possible $(+\hat{\boldsymbol{z}}, -\hat{\boldsymbol{z}})$ orientations, owing to the orientating effect of counterflow.

In conclusion: the first NMR experiments (Ikkala *et al* 1982) on rotating ^{3}He-B in the presence of vortices revealed a *hysteretic transition.* This was subsequently interpreted (for a review, see Salomaa and Volovik 1987) to signal a first-order phase transition between two vortices with *different momentum-space topology.* Later NMR experiments (Hakonen and Nummila 1987) on rotating ^{3}He-B in the vortex-free state revealed a *hysteretic transition* at a critical angular velocity of rotation $\Omega = \Omega^*$, characterised in NMR by $\sin^2\beta = 1$. I find that the latter signals a first-order phase transition as well, currently of the order-parameter $\hat{\boldsymbol{n}}$ texture between the conventional flare-out and the new flare-in textures with the same discrete symmetries but, in the absence of vortices, with *different real-space topology.*

Acknowledgments

I want to thank A D Gongadze, P J Hakonen, Z Janu, G A Kharadze, Y Kondo, J S Korhonen, M Krusius, O V Lounasmaa, O V Magradze, Yu M Mukharsky, K K Nummila, J P Pekola and G E Volovik for useful discussions. This research has been supported through the Award for the Advancement of European Science by the Körber-Stiftung (Hamburg, Federal Republic of Germany) and by the Academy of Finland.

References

Brinkman W F, Smith H, Osheroff D D and Blount E I 1974 *Phys. Rev. Lett.* **32** 584

Gongadze A D, Gurgenishvili G E and Kharadze G A 1981 *Fiz. Nizk. Temp.* 7 821 (Engl. Transl. 1981 *Sov. J. Low Temp. Phys.* 7 397)

Hakonen P J, Ikkala O T, Islander S T, Lounasmaa O V and Volovik G E 1983 *J. Low Temp. Phys.* **53** 425

Hakonen P J, Krusius M, Salomaa M M, Salmelin R H, Simola J T, Gongadze A D, Vachnadze G E and Kharadze G A 1989a *J. Low Temp. Phys.* **76** 225

Hakonen P J, Lounasmaa O V and Simola J T 1989b *Physica* B **160** 1

Hakonen P J and Nummila K K 1987 *Phys. Rev. Lett.* **59** 1006

Hakonen P J and Volovik G E 1982 *J. Phys. C: Solid State Phys.* **15** L1277

Ikkala O T, Volovik G E, Hakonen P J, Bun'kov Yu M, Islander S T and Kharadze G A 1982 *Pis. Zh. Eksp. Teor. Fiz.* **35** 338 (Engl. Transl. 1982 *JETP Lett.* **35** 416)
Jacobsen K W and Smith H 1983 *J. Low Temp. Phys.* **52** 527
Korhonen J S, Janu Z, Kondo Y, Krusius M, Mukharsky Yu M and Gongadze A D 1989 *Report* TKK-F-A653 and to be published
Leggett A J 1973 *J. Phys. C: Solid State Phys.* **6** 3187
Maki K and Nakahara M 1983 *Phys. Rev.* B **27** 4181
Nummila K K, Hakonen P J and Magradze O V 1989 *Europhys. Lett.* **9** 355
Osheroff D D 1977 *Physica* B **90** 20
Salmelin R H, Pekola J P, Manninen A J, Torizuka K, Berglund M P, Kyynäräinen J M, Lounasmaa O V, Tvalashvili G K, Magradze O V, Varoquaux E, Avenel O and Mineev V P 1989 *Phys. Rev. Lett.* **63** 620
Salomaa M M and Volovik G E 1987 *Rev. Mod. Phys.* **59** 533
—— 1989 *J. Low Temp. Phys.* **75** 209
Smith H, Brinkman W F and Engelsberg S 1977 *Phys. Rev.* B **15** 199
Spencer G F and Ihas G G 1982 *Phys. Rev. Lett.* **48** 1118
Theodorakis S and Fetter A L 1983 *J. Low Temp. Phys.* **52** 559
Thuneberg E V 1986 *Phys. Rev.* B **33** 5124
Volovik G E, Gongadze A D, Gurgenishvili G E, Kharadze G A and Salomaa M M 1982 *Pis. Zh. Eksp. Teor. Fiz.* **36** 404 (Engl. Transl. 1982 *JETP Lett.* **36** 489)